Highlights

- Evaluation of LPMO activity on cellulosic substrates of different crystallinity
- SamLPMO10C is more active on celluloses with high crystallinity and accessibility
- Synergism of LPMOs and endoglucanases on NFC production from flax
- First study reporting the effect of a bacterial LPMO in nanocellulose production

Differential activity of lytic polysaccharide monooxygenases on celluloses of different crystallinity. Effectiveness in the sustainable production of cellulose nanofibrils

Susana V. Valenzuela[*1,2], Cristina Valls[3], Viviane Schink[1], Daniel Sánchez[1], M. Blanca Roncero[3], Pilar Diaz[1,2], Josefina Martínez[1,2], F.I. Javier Pastor[1,2]

Department of Genetics, Microbiology and Statistics. Faculty of Biology. Universitat de Barcelona. Av. Diagonal 643, 08028 Barcelona, Spain.

Institute of Nanoscience and Nanotechnology (IN2UB), Universitat de Barcelona, Spain

CELBIOTECH_Paper Engineering Research Group. Universitat Politècnica de Catalunya. Barcelona Tech, 08222 Terrassa, Spain.

*Corresponding autor: susanavalenzuela@ub.edu

ABSTRACT

A series of cellulosic substrates has been produced, treated with lytic polysaccharide monooxygenase (LPMO) from *Streptomyces ambofaciens* (SamLPMO10C), and analyzed by high performance anion exchange chromatography (HPAEC) with pulsed amperometric detection (PAD). The activity of the bacterial LPMO showed high variability depending on the origin and degree of crystallinity of the substrate. Additionally, we tested the effectiveness of SamLPMO10C in the nanofibrillation of flax, a high crystalline agricultural fiber, as a single pretreatment or in combination with cellulases. All pretreatments were followed by a mechanical defibrillation by high-pressure homogenization (HPH) to obtain cellulose nanofibrils (NFC). The combined LPMO-cellulase treatment showed higher fibrillation yield, optical transmittance and carboxylate content than control reactions. Therefore, it could be explored as a promising green alternative to reduce the energy consumption in the production of NFC. To our knowledge, this is the first study reporting the effect of a bacterial LPMO in nanocellulose production.

INTRODUCTION

Lignocellulose is the main source of carbohydrates on Earth, thus its deconstruction and utilization has become one of the most promising target of sustainable industrial processes. Bacterial lytic polysaccharide monooxygenases (LPMO10s) are a specific type of LPMOs classified as Auxiliary Activity enzymes of family 10 (AA10) according to the Carbohydrate-Active enZYmes Database, CAZy (Lombard, Golaconda Ramulu, Drula, Coutinho, & Henrissat, 2014). They were described in 2010 as oxidative enzymes that catalyze the depolymerization of recalcitrant polysaccharides such as cellulose, the most abundant polysaccharide of lignocellulosic materials, and chitin, an ubiquitous polymer in arthropods and fungi (Vaaje-Kolstad et al., 2010; Vaaje-Kolstad, Forsberg, Loose, Bissaro, & Eijsink, 2017). These particular type of LPMOs, together with fungal LPMOs, are thought to act on the crystalline portion of polysaccharides, becoming key players in biomass deconstruction (Johansen, 2016b). Nowadays, LPMOs are a central component of commercial enzymatic cocktails used for the industrial production of lignocellulosic ethanol in several large-scale plants, since they enable the action of other enzymes that can only act if substrates are more accessible (Johansen, 2016a).

LPMOs cleave cellulose leading to the formation of cello-oligosaccharides oxidized at different positions of the glucose ring, aldonic acids when oxidized at the C1 position and/or 4-ketoaldoses at the C4 position (Forsberg et al., 2014). So far, the detection of soluble oxidized products released from phosphoric acid swollen cellulose (PASC) by HPAEC is one of the most suitable method for analyzing C1-oxidized cello-dextrins (Westereng et al., 2013). PASC is described as a cellulose derivate with similar crystallinity than Avicel (Hall, Bansal, Lee, Realff, & Bommarius, 2010; Zhang & Lynd, 2006), and its preparation includes a swelling treatment with phosphoric acid that improves the accessibility to the cellulose chains. Other cellulosic substrates, like regenerated amorphous cellulose (RAC), and starch have been reported as oxidizable substrates for fungal LPMOs (Frommhagen et al., 2017; Lo Leggio et al., 2015), but there are still few reports exploring the effect of cellulose active LPMO10s on substrates different than PASC. Some authors have explored the action of LPMO10s on filter paper or carboxymethyl cellulose, but the standard assay is conventionally performed on PASC (Ghatge et al., 2015; Moser, Irwin, Chen, & Wilson, 2008; Westereng, Arntzen, Agger, Vaaje-Kolstad, & Eijsink, 2017).

Among novel cellulosic resources, the production of NFCs or cellulose nanofibers has focused the attention for the development of renewable materials, because of its exceptional physicochemical properties. NFCs have shown a promising potential in paper and packaging applications, food additives,

personal care products, lightweight composites for aerospace and automotive, building and construction, biomedical, energy and water purification (Karim, Afrin, Husain, & Danish, 2017; Shatkin, Wegner, Bilek, & Cowie, 2014). The term NFC is used to describe an aqueous suspension of cellulose fibers disintegrated until the microfibrils have been released from the plant cell wall. When the concentration of NFC is low, between 0.5 and 2%, the suspension forms a gel-like substance used as an additive for the industrial applications mentioned. To produce NFC the preferred protocol includes a chemical pretreatment of the cellulosic material, followed by an intense high-pressure treatment in a homogenizer or a microfluidizer. The pretreatment reduces the high energy requirements to break down the fiber's structure and helps to avoid clogging of the system by fiber entanglement (Spence, Venditti, Rojas, Habibi, & Pawlak, 2011). Although chemical pretreatments as acid based or 2,2,6,6-tetramethylpiperidine-1-oxyl (TEMPO)-mediated oxidation seem to be effective, their toxicity and side effects rule out their extensive use. The use of glycosyl hydrolases in combination with mechanical shearing and HPH has opened novel applications in material sciences, as it can improve the final properties of the product without collateral toxic effects (Pääkkö et al., 2007). In this direction, recently, a few studies with oxidases, have shown the potential of fungal LPMOs as a sustainable and green pretreatment method in the production of NFCs (Hu, Tian, Renneckar, & Saddler, 2018; Karim et al., 2017).

We believe that LPMO10s can be developed as a cheap and easy to manage alternative component in pretreatments, as they can be cloned and expressed in *Escherichia coli*, avoiding codon optimization and eucaryotic fermentation. In this context, we analyzed the activity SamLPMO10C from *Streptomyces ambofaciens* on flax pulp as a non-woody material to assess the modification produced in the fibers and evaluated its contribution to NFC production. A recent study suggested that SamLPMO10C was active on flax, but not in others pulps tested (Valenzuela, Ferreres, Margalef, & Pastor, 2017). Therefore, as flax is a highly crystalline pulp compared with other cellulosic materials, firstly, we decided to evaluate the influence of substrate crystallinity on the enzyme activity. Secondly, for the production of NFC, we have assayed three different pretreatments: enzymatic hydrolysis, LPMO10-mediated oxidation, and combination of the two enzymatic activities. All pretreatments were followed by a mechanical defibrillation by HPH to produce NFCs. Physicochemical characteristics of the fibers indicated that the combination of LPMO10s with cellulases is effective in facilitating the production of NFCs and therefore,

it could be a promising green alternative as a pretreatment for the subsequent fibrillation of cellulose in the production of cellulosic nanomaterials.

RESULTS and DISCUSSION

Preparation of cellulosic substrates

PASC has been routinely considered as the preferred substrate of cellulose active LPMOs. PASC is a cellulosic derivate, obtained by treatment of Avicel with phosphoric acid, which shows a crystallinity index (CrI) between 56-91% depending on the severity of the treatment and the method used in the analysis (Park, Baker, Himmel, Parilla, & Johnson, 2010). Since PASC preparation is a cellulose swelling (heterogeneous) process, the quality of PASC has great variability, depending on operation conditions such as swelling and blending times, acid concentration, and efficiency in removing cellulose lumps (Zhang, Cui, Lynd, & Kuang, 2006). We prepared several different cellulosic substrates in order to analyze the behavior of LPMOs on celluloses of different degree of crystallinity. All these substrates were obtained from a highly pure cellulose, to avoid interferences of components like lignin or hemicellulases that are present in most of cellulosic sources. Attending to this, we obtained and characterized four different Avicel derivatives using different combinations of acidic solvent concentration and variations of the incubation temperature. The common swollen cellulose PASC and the amorphous cellulose RAC, precipitated from the dissolved homogeneous cellulose, were prepared using 70% and 85% phosphoric acid respectively, as described elsewhere (Zhang et al., 2006). Additionally, a method for reaching intermediate degrees of crystallinity from Avicel was applied using 76% and 78% phosphoric acid, to obtain two more cellulosic substrates that we denominated C-76 and C-78 (Hall et al., 2010). One of the more crystalline cellulose described is nanocellulose of bacterial origin, also known as bacterial cellulose (BC). This is a pure cellulose substrate, which can be obtained from different species as an extracellular secreted matrix. We produced films of BC from *Komagataeibacter xylinus* by static culture, which were purified and disintegrated as described, to be also tested as a substrate for LPMOs.

All the cellulosic substrates were analyzed by optical microscopy and scanning electronic microscopy (FESEM), Fig. 1, and their CrI was determined by X-ray diffraction (XRD) (Table 1). As expected, BC showed the highest crystallinity among the celluloses analyzed (CrI 95.7% ± 0.5). FESEM analysis of BC showed a cellulose framework with a completely different structure from the other substrates analyzed, with narrow fibers seen at high magnification (Fig. 1). Nanostructures of cellulose were more clearly observed in BC using a magnification of 20000X while none of the other samples showed these structures (Fig. SI 1). Treatment of Avicel with phosphoric acid, decreased crystallinity of samples, in an extent correlated to the severity of the treatment (acid concentration and temperature).

However, PASC (CrI 93% ± 1.8) did not show a significative CrI difference with Avicel (CrI 92.4% ± 1,1), although the acid treatment diminished PASC particle size to around 1 microns, in contrast with non-treated Avicel, that showed particles more than 10 times bigger, as noted in the optical microscopy (Fig. 1), and in agreement with PASC description elsewhere (Zhang et al., 2006). The regenerated cellulose RAC and C-78 were the most amorphous substrates characterized (CrI 67.4% ± 1.6 and 49.9% ± 4.3 respectively), where the crystalline structures shown by Avicel could not be observed at all by optical microscopy or FESEM. On its side, sample C-76 showed CrI of 88.1% ± 5, an intermediate value between highly crystalline and amorphous cellulose substrates. In the FESEM analysis it is possible to observe a slightly change in the structure of cellulose of C-76 compared with Avicel and PASC. The X-ray diffraction pattern of the different cellulosic substrates prepared is shown in Fig. SI 2.

The determination of the crystallinity by XRD using the peak height method was described by Segal et al. (Segal, Creely, Martin, & Conrad, 1959) as a semi-quantitative evaluation of the amounts of amorphous and crystalline cellulosic components in a sample. The analysis is very useful because it allows a rapid comparison between samples, and it is the most widely used method in the literature to measure the CrI of commercial celluloses (Park et al., 2010). Using this method, the absolute value of crystallinity of Avicel is usually > 90% (Hall et al., 2010; Park et al., 2010), far from the 60% determined when the crystallinity is analyzed by NMR. Nevertheless, using substrates with a wide range of crystallinity, the NMR method also has inconvenience in the resolution of the C4 carbon signal within a reasonable acquisition time in samples with low crystallinity (Hall et al., 2010). In our work, the combination of the analyses of the treated cellulosic samples by X-Ray and FESEM provided a simple choice to compare the structure and crystallinity of the cellulosic substrates developed.

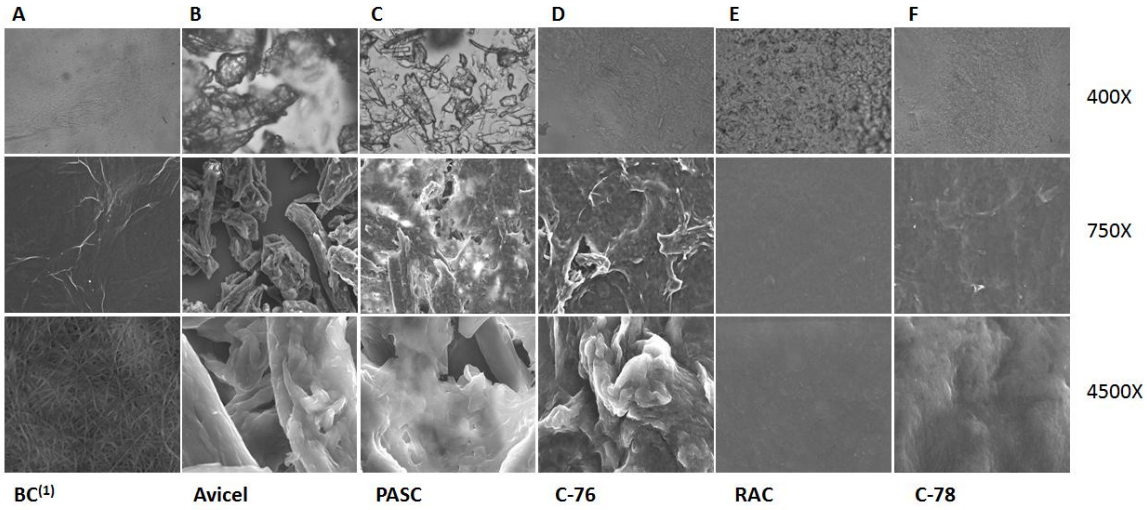

Figure 1. Cellulosic substrates. Optical microscopy (1st row) and FESEM microscopy (2nd and 3rd rows) of BC (A), Avicel (B), PASC (C), C-76 (D), RAC (E), and C-78 (F).
(1), BC FESEM image was taken with 8000X instead of 4500X

Table 1. CrI of the cellulosic substrates, measured by XRD.

Cellulosic substrate	CrI (%)
BC *K. xylinus*	95.7 ± 0.5
Avicel	92.4 ± 1.1
PASC	93.0 ± 1.8
C-76	88.1 ± 5
RAC	67.4 ± 1.6
C-78	49.9 ± 4.3

Optimization of enzymatic activity

SamLPMO10C (Uniprot, A3KKC4) was recently characterized as a cellulose active LPMO which shows activity on paper pulps (Valenzuela et al., 2017). We explored the supplementation of H_2O_2 as a source of oxygen in the enzymatic assay, as proposed recently (Bissaro et al., 2017), and compared with the activity determination by the typical assay using molecular oxygen as co-substrate of the enzyme. The release of cellobionic acid was monitored to quantify enzymatic activity of SamLPMO10C. Addition of 20 μM H_2O_2 gave rise to a dramatic increase in the release of cellobionic acid and other oxidized oligosaccharides from PASC (Fig. 2), similarly to that reported for ScLPMO10C (Bissaro et al.,

2017). A similar effect was observed on flax pulp, where the activity on this substrate was approximately 3-fold increased. The addition of H_2O_2 to trigger enzyme reaction could improve the efficiency of LPMO application in biorefining processes of lignocellulose, since the aeration at large scale, together with the delivery of electrons, are considered major challenges (Bissaro et al., 2017). Additionally, the effect of SamLPMO10C on PASC and flax pulp at different concentration was also tested. SamLPMO10C showed an increase in cellobionic acid production when the substrate concentration was increased (Fig. 2). Therefore, even when the liberation of cellobionic acid from the substrates is very low, (less than 100 mg/l), as the enzyme is probably attacking highly specific zones on the fiber, it is not saturated by the substrate even at the high concentrations used. Recently, Villares et al. (Villares et al., 2017) suggested that the action of LPMO on cellulose fibers is a mechanism that create nicking points that decrease cohesion of the fibers. This structural modification can create new entry points for the attack of other enzymes, such as endoglucanases. Thus, if these fibers are not enough exposed in the surface, then more substrate would be needed to saturate the active site of the enzyme.

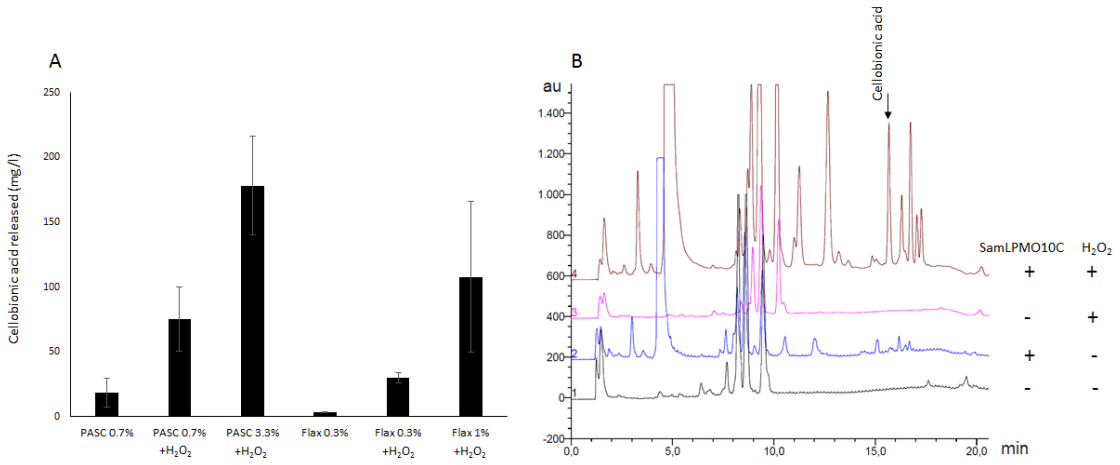

Figure 2. Cellobionic acid release by SamLPMO10C. A, Evaluation of substrate concentration and hydrogen peroxide in the oxidative reaction. B, Analysis by HPAEC-PAD of products released from PASC by SamLPMO10C.

Activity on cellulosic substrates

To evaluate the effect of substrate crystallinity on SamLPMO10C activity, we performed enzymatic assays on the cellulosic substrates of different CrI previously prepared. SamLPMO10C showed maximum activity, measured as cellobionic acid released, on BC, which is the most crystalline substrate

used (Fig. 3). The following preferred substrates were PASC and C-76, on which of SamLPMO10C showed similar activity (around 60 and 45% of that found on BC), while lower activity was observed on Avicel. These results were surprising as PASC and Avicel show a similar CrI and have the same cellulose source. Nevertheless, the pre-treatment of phosphoric acid done for PASC production disrupted the particle size, as seen by Optical Microscopy, thus probably enhancing the surface contact with the enzyme. As it was shown before, substrate concentration was important for the product release. Therefore, diminishing size particle was probably causing the same effect by increasing the contact surface and as a result, increasing the critical target zones for the action of the enzyme. The lowest activity of SamLPMO10C was found on RAC and C-78, which are the less crystalline substrates evaluated. Excluding Avicel, our results indicate that there is a correlation between the crystallinity of cellulose and the activity of SamLPMO10C, and are in accordance with the common recognition that the LPMOs act first on the microcrystalline substrates, making the polymers accessible to the glycoside hydrolases (Johansen, 2016b; Nakagawa, Eijsink, Totani, & Vaaje-Kolstad, 2013). On the contrary, it has been described that cellulases show a steep change in activity on Avicel treated with phosphoric acid in narrow range (75–80%), showing more activity when more amorphous the substrates are. The correlation between the CrI and the initial hydrolysis rate in cellulases is reported to show a continuous decrease in rate as crystallinity increases (Hall et al., 2010).

Our results show that, besides crystallinity, factors such as the surface area of the substrate seem also to affect the effectiveness of LPMOs. As the BC showed also a completely different nanostructure than the other substrates, this could be causing the same effect of exposing better the fibers that are susceptible for the LPMO action. Our results are in agreement with those reported by Hu, Arantes, Pribowo, Gourlay, & Saddler, (2014) showing the important effect of crystalline cellulose accessibility on LPMO activity. Crystalline regions of cellulose should be accessible in the surface of the polymer. In accordance with our results, the quoted report also shows that a fungal LPMO shows higher absorption to PASC than to Avicel. To better understand the effect of SamAA10C on the cellulosic substrates, the CrI of PASC after treatment with the enzyme was analyzed, although no significant changes were detected. A recent study has described a slight decrease in the crystallinity of a softwood kraft pulp after the treatment with a fungal LPMO, mainly attributed to the modification of the inaccessible surface area by the disruption of specific points of the fibers (Villares et al., 2017). In our case, as the technique employed measures the CrI of the whole sample, this change may become unnoticed.

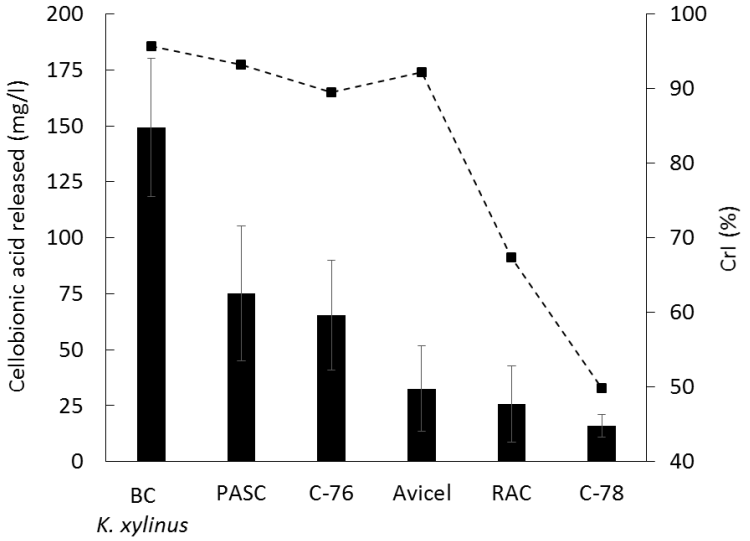

Figure 3. Activity of SamLPMO10C vs. substrate crystallinity. Correlation between cellobionic acid release by SamLPMO10C (bars) and the crystallinity degree of the cellulosic substrates (dashed line).

Synergy with Endoglucanases

The efficient degradation of cellulosic materials is still challenging because of the huge battery of different enzymes required to act in a synergistic manner. Cellulolytic hydrolytic enzymes can be classified according to their modes of action as endoglucanase, exoglucanase, or β-glucosidase (Lombard et al., 2014). In addition, other complementary enzymes like LPMOs and expansins seem to trigger and/or improve the cooperative action of cellulases in cellulosic degradation (Bunterngsook, Mhuantong, Champreda, Thamchaipenet, & Eurwilaichitr, 2014; Eibinger, Sattelkow, Ganner, Plank, & Nidetzky, 2017a).

The synergism of SamLPMO10C with Cel9B, a processive endoglucanase from *P. barcinonensis* (Chiriac et al., 2010), on depolymerization of flax pulps was explored. Flax pulps were pretreated with SamLPMO10C for 72 h, following treated with Cel9B for 15 min or 18 h and the reducing sugars produced were quantified (Fig. 4). A higher amount of released sugars was found than that produced by the only activity of Cel9B, while, as expected, SamLPMO10C did not release reducing sugars from flax pulp. The results indicate a synergistic action of the two enzymes, which was more evident when the cellulase reacted overnight. Maximum synergism effect was achieved in a range between 0.5-2 μM Cel9B, which produced 3-fold higher amount of reducing sugars. Although stimulation of cellulase activity has been reported for several combinations of cellulases and LPMOs, important

differences have been described in terms of substrate, dose, time of incubation and type of cellulase (endo or exo hydrolysis) (Eibinger, Sattelkow, Ganner, Plank, & Nidetzky, 2017b; Moser et al., 2008; Vermaas, Crowley, Beckham, & Payne, 2015). Hu et al. (2014) analyzed the substrate factors influencing synergism between a fungal LPMO and a cellulase cocktail on depolymerization of biomass. They showed an LPMO boosting effect that was affected by cellulose accessibility. A correlation between the synergy of the fungal LPMO with cellulases and the ratio of accessible crystalline cellulose to amorphous cellulose was found. Similarly to these studies, our results suggest that LPMOs create more reactive sites for cellulases on recalcitrant crystalline regions, but this areas should be accessible in the surface of the polymer. Our results show that SamLPMO10C pretreatment favors flax pulp hydrolysis. The utilization of LPMOs in industrial applications requires the optimization of application conditions, enzyme dosage and ratio of cellulases and LPMOs, to save excessive costs of enzyme.

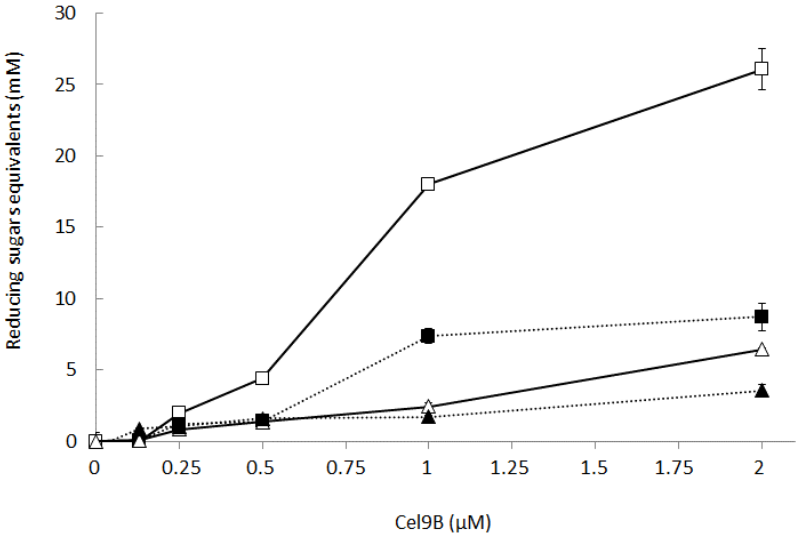

Figure 4. Cel9B activity on flax with (continuous line) or without (doted line) a 72 h pretreatment with SamLPMO10C. Reducing sugars were detected after the incubation with different concentrations of Cel9B for 15 min (triangles) or 18 h (squares).

Nanocellulose from flax pulp

NFC is usually manufactured from paper pulp by a mechanical treatment preceded by a chemical pretreatment, including acid or TEMPO-mediated oxidation (Fillat et al., 2018; Saito, Nishiyama, Putaux, Vignon, & Isogai, 2006). Nevertheless, to avoid the use of toxic chemicals, enzymes as cellulases, hemicellulases and recently, LPMOs, have shown potential use for NFC production from paper pulps in an environmentally friendly process (Hu et al., 2018; Karim et al., 2017; Villares et al., 2017).

Our work was focused on assessing the potential of SamLPMO10C to enhance nanofibrillation of flax pulp. In order to find a suitable pretreatment, we use the oxidative enzyme in two different procedures: single application of SamLPMO10C (S treatment) and in combination with endocellulase Cel9B (S-C9 treatment), which as above shown act synergistically. Besides, single application of Cel9B was also evaluated (C9 treatment), as a control of an enzyme that shows a refining effect on flax pulps (Garcia-Ubasart, Torres, Vila, Pastor, & Vidal, 2013). After the pretreatment, pulps were subjected to a high-pressure homogenization (HPH) and the properties of the material obtained were evaluated. All the treatments where compared with a control processed in the same conditions, but in the absence of enzymes (Flax). A summary of the results is shown in Table 2 and Fig. 5.

Mechanical fibrillation used to produce NFC gives an inhomogeneous material, containing nanofibrillated, partially and non-fibrillated material (Chinga-Carrasco, 2011). The nanofibrillation yield is usually determined by low speed centrifugation, where nanofibers are found in the supernatant, and non-fibrillated and partially fibrillated material remains in the precipitate. S-C9 was the most effective treatment, with a successful conversion of flax pulps to NFC, with a final yield of 24.3% nanofibers. C9 treatment also showed effectiveness to nanofibrillate flax, but in a lower extent (17.0% yield). A smaller amount of nanofibers were found in S samples (12.7%). On the other, 2.1% nanofibers were produced from flax without enzymatic treatment. The results show that incubation with LPMO and cellulase was efficient as a pretreatment to increase the production of nanofibrillated material. An image of the nanofibrillated cellulose obtained with S-C9 pretreatment is shown in Fig SI 4, where a network of nanofibrils surrounding a fiber of greater dimensions can be observed, while in control sample no nanofibrils can be seen.

Table 2. Characteristic parameters used to analyze the production of the NFC: Yield, Transmittance, Carboxylic acid content and Zeta potential. Cellobionic acid released from fibers was added as an indirect measure of the effect of SamLPMO10C on flax.

	Yield of NFC (%)	Transmittance at 700 nm (%)	Cellobionic Acid release (mg/l)	COOH (µmol/g)	Zeta potential (mV)
Flax	2.1±3	31.8	0±0	16±5.5	-23.2±0.4
C9	17.0±1.7	37.1	0±0	24±0.7	-37.1±0.5
S	12.7±0.5	39.1	10.2±1.0	37±1.4	-25.7±1.3
S-C9	24.3±0.5	45.4	21.6±1.9	36±0.1	-37.2±1.6

286

As a complementary assay to determine the degree of nanofibrillation of the cellulose, we measured the UV-vis transmittance of an aqueous suspension of samples after HPH. As the transmittance is wavelength-dependent because light scatters more when the wavelength approaches the diameter of the particles, increase of transmitance can be an indirect evaluation of the yield (Saito, Kimura, Nishiyama, & Isogai, 2007). The transmittance at 700 nm of the homogenized flax samples is shown in Table 2, while the UV−vis transmittance spectra is shown in Fig. SI 3. Higher values were obtained when treating with the two enzymes, S-C9, and the less translucent suspension was obtained in the sample without enzyme treatments. The transmittance spectra of C9 and S samples was lower, corroborating that the combined application of the two enzymes is more effective to enhance fibrillation of fibers. The results indicate that SamLPMO10C is suitable for enhancing the yield of the NFC production when is used in combination with cellulases. The degree of nanofibrillation of flax obtained is far from that reported for chemical pretreatments with TEMPO, where yield values of about 70% are achieved (Chaker, Mutje, Vilaseca, & Boufi, 2013). Nevertheless, it has been shown in papermaking, that a high percentage of fibrillation is not essential to produce a significant increase in the paper's mechanical properties, since this is easily compensated by enhancing the proportion of NFC applied as additive, allowing a reduction on the utilization of the harmful reactants used in chemical pretreatments (Delgado-Aguilar et al., 2015). Moreover, in our case, the low content of hemicelluloses of the bleached flax pulp used, around 4%, (Beltramino, Roncero, Vidal, & Valls, 2018) may also have hindered the fibrillation process (Besbes, Alila, & Boufi, 2011; Iwamoto, Abe, & Yano, 2008).

Oxidative cleavage of cellulose by LPMO leads to the formation of oxidized glucose units at different positions, resulting in the formation of aldonic acids at the C1. The release of cellobionic acid in the supernatant of the enzyme pretreatments was quantified by HPAEC. The peak of cellobionic acid was only observed when SamLPMO10C was included in the pretreatments (Fig. 5). The peak's area was higher in S-C9 samples, probably because of the synergy showed between these two enzymes. As expected samples of Flax and C9 did not show cellobionic acid. On the other hand, the COOH content of pulps (non-fibrillated fraction of flax) was measured by the methylene blue absorption method, showing an increase in the carboxylic acid content in those samples oxidized by SamC (S and S-C9). Net values of these quantifications are reported in Table 2. In TEMPO functionalization, the repulsive forces of the ionized carboxylate groups produced by the chemical agent facilitates the separation of nanofibrils within the fibers, which overwhelm the hydrogen bonds holding them together (Missoum, Belgacem, & Bras,

2013). Hence, the oxidation carried out by SamLPMO10C could produce a similar effect, and make easier the fibrillation.

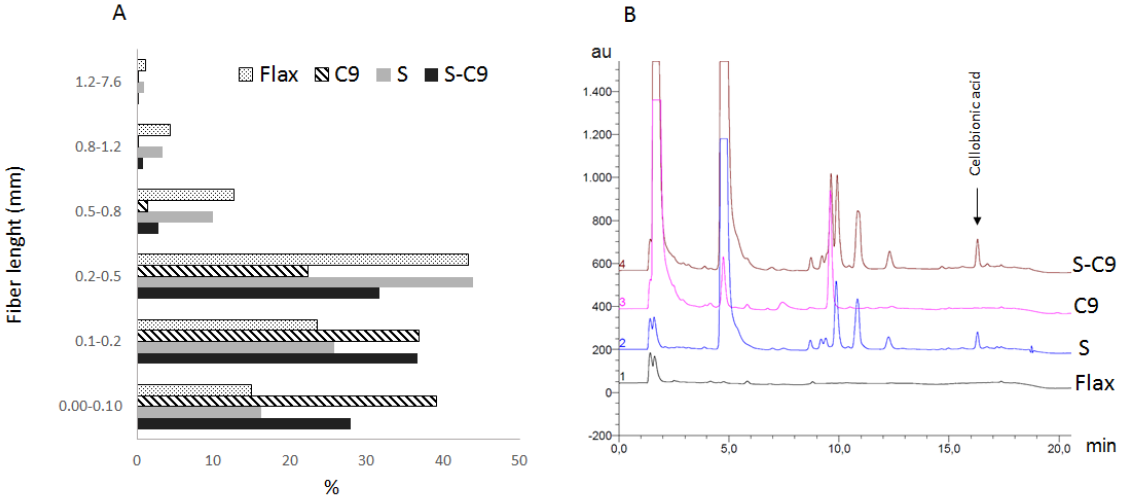

Figure 5. Length fiber distribution of fiber suspension (A) and HPAEC analysis of supernatants (B) after enzymatic pretreatments. Control (Flax), Cel9B (C9), SamLPMO10C (S), and SamLPMO10C + Cel9B (S-C9) pretreatments. The standard deviation of the length fiber distribution was less than 2% in all cases.

Other complementary assays, where performed to characterize better the cellulosic materials produced after the different treatments. Electrophoretic mobility of particles, expressed as zeta potential is a good indicator of colloidal stability of suspensions obtained after HPH. The suspension of samples without enzyme pretreatment had a stability (-23.2 mV ±0.4) similar to that of NFC reported by Hu et al. (2018), but lower than that found on nanocrystalline cellulose obtained from cotton linters (Beltramino, Blanca Roncero, Vidal, & Valls, 2018). Whereas S pretreatment did not affect this value, enzymatic pretreatment with C9 increased the stability of the suspension (-37.2 mV ±1.6). NFC production is expected to produce structural changes in the cellulose, by disrupting large fibers in order to release nanofibers. For this reason, to assess the effect of each treatment on cellulose, the degree of polymerization (DP) of the samples was determined after the HPH stage. The DP of the control sample was 2488 and in all cases the enzymatic treatments caused a decrease in DP. The combined enzymatic treatment S-C9, showed the more dramatic decrease (68%), followed by the C9 treatment (58%). Surprisingly, even when S treatment was not able to efficiently produce NFC, it caused a modification in the fibers that gave rise to a material with lower DP (decrease of 28%). This corroborates that although the SamLPMO10C pretreatment was less effective in producing NFC, it induced significant modifications in the fibers. Fiber length of the treated pulps was assessed by Kajaani's assay (Fig. 5). It shows how the

enzymatic pretreatment affect fibers length distribution. Enzyme pretreated fibers show higher quantity of short fibers, shorter than 0.2 mm, and lower quantity of fibers longer than 0.5 mm. The most significant decrease in fiber length was produced in samples pretreated with cellulase, either alone (C9) or in combination with the LPMO (S-C9). In these samples, the amount of fibers lower than 0.2 mm increased 96% and 67% respectively. The lower effect produced by S-C9 with respect to C9 alone may be explained by higher nanofibrillated material of narrower diameter, not detected by the Kajaani's apparatus. As well, scanning electron microscopy (FESEM) suggested that the surface morphology of the fibers change mostly when cellulases were present, as a single treatment or in S-C9 treatment, where the smoothness of the surface of the fiber seems to be disrupted or peeled after the enzymatic treatments (Fig. SI 4).

The results suggest that LPMO mediated treatments have the potential to induce the fibrillation of paper pulp in combination with cellulases, therefore they could be explored as an environmentally friendly alternative to reduce the energy consumption of the HPH used in the production of NFC. This is the first study reporting the combined effect of an LPMO10 and a cellulase in nanocellulose production.

Materials and methods

Cellulosic substrate preparation

Bacterial cellulose (BC): *Komagataeibacter xylinus* was grown on the Hestrin and Schramm (HS) medium, containing 20 g/L glucose, 20 g/L peptone, 10 g/L yeast extract, 1.15 g/L citric acid, 6.8 g/L Na_2HPO_4, pH 6 to produce BC. Inoculum for culture was prepared by transferring *K. xylinus* cells grown on HS–Agar to HS liquid medium. After shaking vigorously, the resulting cell suspension was used to inoculate (1:40) 10 cm–Petri dishes containing 40 mL of HS medium. The cultures were statically incubated at 25–28°C for 7 days, because the static incubation gives rise to BC with a higher CrI, compared with the agitated fermentation (Czaja, Romanovicz, & Brown Jr, 2004). After incubation, BC pellicles generated in the air/liquid interface of the culture media were harvested, rinsed with water and cleared by an incubation in 1% NaOH at 70°C overnight. Finally, the BC pellicles were thoroughly washed in deionized water until the pH reached neutrality. To obtain the BC pulp, pellicles were mechanically cut into small pieces and disrupted with a homogenizer (Homogenizing System UNIDRIVE X1000).

PASC (Phosphoric Acid Swollen Cellulose): Avicel® PH-101 (Fluka) was treated with 70% of H_3PO_4 according to Wood, (Wood, 1988), using centrifugation for the sedimentation of the cellulose instead of decantation during the washing process.

RAC (Regenerated Cellulose): Avicel® PH-101 was treated with 85% of H_3PO_4 according to Zhang and col. (Zhang et al., 2006).

C-76 and C-78: The preparation of these cellulosic substrates was performed by the method described previously (Hall et al., 2010), using 76 and 78% of cold H_3PO_4 respectively for treating the Avicel® PH-101.

All the resulting substrates were resuspended in MiliQ water. Dry weight of samples was measured in triplicate by drying 10 ml of cellulosic suspension at 60 ºC until constant weight.

Characterization of cellulosic substrates

The crystallinity index (CrI) of different cellulosic substrates were measured by X-ray diffraction (XRD) method (Segal et al., 1959), where the ratio between the height of the crystalline peak and the height of the minimun is used to calculate the CrI. This method allows a rapid evaluation of cellulose samples and is very appropriate for comparing the relative differences between them (Park et al., 2010). Samples were dried directly on an aluminum plate of 32 mm of diameter and 3.0 mm of thickness, that were mounted in standard sample holders for bulk samples of thickness ≤ 7 mm (PW1812/00). A PANalytical X'Pert PRO MPD Alpha1 powder diffractometer in Bragg-Brentano θ/2θ geometry of 240 millimetres of radius with Cu Kα1 radiation (λ = 1.5406 Å) at 45 kV and 40 mA, focalizing Ge (111) primary monochromator, with sample spinning at 2 revolutions per second, fixed divergence slit of 0.25º was used. The measurement range (2θ) was from 2 to 50º with step size of 0.033º and measuring time of 100 seconds per step. To calculate the CrI of cellulose from the XRD spectra, the Peak Height method used elsewhere was employed (Segal et al., 1959). Surface of cellulosic substrates and disintegrated pulp after enzymatic treatments and homogenization was analyzed by optical microscopy (digital Microscope Olympus CX31) and by FESEM (JSM 7100 F) using a LED filter and a backscattered electron detector (BED).

Expression of SamLPMO10C and Cel9B and purification by polysaccharide-binding

E. coli BL21 star (DE3) harvesting pET11samLPMO10C (Valenzuela et al., 2017) or pET28cel9B (Chiriac et al., 2010) were cultured in LB antibiotic supplemented medium at 37°C, and

induced by 0.5 mM isopropyl β-D-1-thiogalactopyranoside (IPTG) at $O.D._{600nm}$ = 0.8. After cultivation at 21°C for 18 h, cell pellets were collected by centrifugation, resuspended in 1/30 of the initial volume with 50 mM Tris-HCl pH 7, and cells were lysed using PANDA GEA 2000 homogenizer at 800 bar. 50 ml of cleared cell extracts were mixed with 5% (w/v) Avicel® PH-101 (Fluka), in Falcon tubes with gentle rotary shaking for 1 h at 4 ºC. Following, samples of SamLPMO10C were purified as described previously (Valenzuela et al., 2017), with some modifications: To collect bound proteins, a centrifugation of 5 min at 14,000 x g was used to separate the pellet of insoluble polysaccharides with adsorbed enzymes. The pellets were sequentially washed 3 times with fresh buffer and centrifuged to remove non-specifically bound proteins. To elute adsorbed enzymes, pellets were washed with 2 volumes of 1 M glucose, for 30 min each, at 4 ºC with gentle rotary shaking. Then, samples were centrifuged at 14,000 x g for 5 min to separate supernatants (with eluted SamLPMO10C) from pellet. For Cel9B the purification were performed according to the method described elsewhere (Chiriac et al., 2010). Homogeneity of samples were analyzed by sodium dodecyl sulphate polyacrylamide gel electrophoresis (SDS-PAGE).

Copper saturation

Purified SamLPMO10C was saturated with copper by incubation with a 4-fold molar excess of $CuSO_4$ for 30 min at room temperature. Excess copper and glucose were removed by desalting the proteins using a PD-10 desalting columns (GE Healthcare) equilibrated with 20 mM MES buffer, pH 5.5. The concentration of desalted Cu_2^+-saturated SamLPMO10C was measured with NanoDrop® ND-1000 (NanoDrop Technologies, Inc), using an extinction coefficient (ε) at 280 nm of 75775 M_1 cm_1, and the enzyme solution was stored at -20 ºC until use.

Degradation reactions

Standard reactions were carried out by mixing between 0.3 to 3.3 mg of substrate with 5 μM of Cu_2^+-saturated SamLPMO10C, 2 mM ascorbic acid and 20 μM of H_2O_2 in a final volume of 0.1 ml in 1.5 ml microcentrifuge tubes. All reactions were performed in 10 mM of ammonium acetate pH 5.5, and incubated for 72 h at 50 ºC with shaking in an Eppendorf Thermomixer unless stated otherwise. Control reactions where the LPMO, or H_2O_2 were excluded from the reaction solution were run in the same manner. All reactions were performed in duplicates at least three times.

Activity detection

For sample preparation, after removing insoluble substrates by centrifugation, supernatants were centrifuged and diluted in water 1/20 and analyzed by HPAEC-PAD using Dionex GS50, gradient pump, Dionex AS50 Autosample and electrochemical detector Waters 2465 as described previously (Westereng et al., 2013) with some modification. In brief, a 40-µL sample was injected on a CarboPac PA1 2 × 250 mm analytical column (Dionex). Cello-oligosaccharides were eluted at 0.25 ml/min using a stepwise linear gradient from 100% eluent A (0.1 M NaOH) toward 10% eluent B (0.6 M NaOAc in 0.1 M NaOH) 10 min after injection and 40% eluent B 15 min after injection, followed by a 5 min exponential gradient to 100% B. The column was reconditioned between each run by running initial conditions for 10 min. Standards were generated using 1, 2, 4 and 8 µg/mL cellobiose and cellobionic acid.

Synergysm study

Synergy between LPMO and endocellulases was examined in a sequential reaction, which include (or not) a pretreatment of flax pulps with SamLPMO10C before the action of endoglucanase Cel9B. Flax pulps were incubated at 50 ºC for 72 h with the LPMO as described above. Then, the enzyme was inactivated by heating at 95 ºC for 5 min. The cellulase Cel9B was added in a second step and incubated also at 50ºC. Samples were withdrawn at 15 min and 18 h and inactivated at 95 ºC for 5 min. Solid material was removed by centrifugation at 12,000 x g for 5 min and cleared supernatant was analyzed by DNS to quantify the reducing sugars liberated (Miller, 1959).

Preparation of nanocellulose

Flax ECF bleached fibers were provided by Celesa (Spain). Prior to fibrillation, the starting pulp was prerefined by Valley beating for 40 min until the beating degree of flax pulp was 39.5 °SR. For the treatments, 5 g of oven dried pulp (o.d.p) was diluted in 500 ml of MiliQ water and disintegrated for 1 h at 11,200 rpm with a homogenizer (Homogenizing System UNIDRIVE X1000). After, the following treatments were applied: for Cel9B treatment (C9), 1 g of disintegrated pulp was treated for 18 h with 10 U of enzyme in 50 mM KOAc buffer pH 5.5; for SamLPMO10C (S), 1 g of disintegrated pulp was treated with 10 mg of SamLPMO10C for 72 h in 20 mM of ammonium acetate pH 5.5 with 2 mM ascorbic acid and 20 µM of H_2O_2. For the synergy study (S-C9), 1 g of disintegrated pulp was treated with SamLPMO10C as described, and after 72 h of reaction, the enzyme was inactivated in a water bath 100 °C for 5 min. Then 10 U of Cel9B were added and the reaction took place for 18 h. For control reaction, 1 g of disintegrated pulp was incubated in all the buffer components for 72+18h at the same

conditions. All reactions were incubated at 50 °C with shaking (120 rpm) in a water bath. For the fibrillation, samples were diluted to a concentration of 0,5% and homogenized through the PANDA GEA 2000 homogenizer by 5 passes at 300 bar and 10 passes at 600 bar.

Characterization of NFCs

The yield of fibrillation was calculated after centrifuging samples of 10 ml with 0.1% of solid content at 2,200 x g for 20 min, removing the supernatant (containing the nanofibrillated fraction) and drying pellet (C) at 85 °C until constant weight.

$$Yield = \left(1 - \frac{C\ (g)}{0.01\ g}\right) \cdot 100\ \%$$

Transmittance measurements were measured on samples with 0.1% of solid content. Samples was introduced in quartz cuvettes and the transmittance was obtained with a T92+ UV spectrophotometer (PG instruments) set in the range between 400 and 800 nm. MiliQ water was used as blank (Saito et al., 2007). The cellobionic acid release of each treatment was analyzed by HPAEC, as described above. Carboxyl groups were determined by measuring Methylene Blue absorption onto cellulose fibers (Davidson, 1948). Electrophoretic mobility of aqueous NFC suspensions (zeta potential) was determined using a Zetamaster model ZEM (Malvern Instruments, UK). Data were averaged over 12 measurements. All samples were analyzed at room temperature. NFC viscosity was determined according to ISO 5351:2010. The degree of polymerization was calculated from the intrinsic viscosity (Ƞ), using the equation of (SCAN-CM15:88): DP0.085= 1.1. Cellulose fiber length of initial, LPMO , cellulase and LPMO/cellulase-treated (C) fibers was measured in accordance with Technological Association of the Pulp and Paper Industry (TAPPI) Standard T271 using a Kajaani FS300 fiber analyzer (Metso Automation, Finland).

Funding Statement

This work was financed by the Scientific and Technological Research Council (MINECO, Spain), grant BIOFABCEL CTQ2017-84966-C2-2-R, FILMBIOCEL CTQ2016-77936-R, BIOPAPµFLUID CTQ2013-48995-C2-1-R and CTQ2013-48995-C2-2-R, by the Ajut a la Recerca Transversal Convocatòria ART 2017, by the Pla de Recerca de Catalunya, grant 2014SGR-534, 2017SGR-30, by the ‘‘Fondo Europeo de Desarrollo Regional FEDER’’ and by the Generalitat de

Catalunya, “Xarxa de Referència en Biotecnologia” (XRB). Special thanks are also due to the Serra Húnter Fellow to Cristina Valls.

Ethical statement

This article does not contain any studies with human participants or animals performed by any of the authors.

Acknowledgments

We thank the Serveis Cientifico-Tècnics of the University of Barcelona for technical support in XRD and HPAEC-PAD analysis.

493 References

494 Beltramino, F., Blanca Roncero, M., Vidal, T., & Valls, C. (2018). A novel enzymatic approach to
495 nanocrystalline cellulose preparation. *Carbohydrate Polymers*, *189*, 39–47.
496 https://doi.org/10.1016/J.CARBPOL.2018.02.015

497 Beltramino, F., Roncero, M. B., Vidal, T., & Valls, C. (2018). Facilitating the selection of raw materials:
498 Evaluation of the effects of TCF and ECF bleaching sequences on different wood and non-wood
499 pulps. *Afinidad*, *75*(582). Retrieved from
500 https://www.raco.cat/index.php/afinidad/article/view/338228

501 Besbes, I., Alila, S., & Boufi, S. (2011). Nanofibrillated cellulose from TEMPO-oxidized eucalyptus
502 fibres: Effect of the carboxyl content. *Carbohydrate Polymers*, *84*(3), 975–983.
503 https://doi.org/10.1016/J.CARBPOL.2010.12.052

504 Bissaro, B., Røhr, Å. K., Müller, G., Chylenski, P., Skaugen, M., Forsberg, Z., … Eijsink, V. G. H.
505 (2017). Oxidative cleavage of polysaccharides by monocopper enzymes depends on H2O2. *Nature*
506 *Chemical Biology*, *13*(10), 1123–1128. https://doi.org/10.1038/nchembio.2470

507 Bunterngsook, B., Mhuantong, W., Champreda, V., Thamchaipenet, A., & Eurwilaichitr, L. (2014).
508 Identification of novel bacterial expansins and their synergistic actions on cellulose degradation.
509 *Bioresource Technology*, *159*, 64–71. https://doi.org/10.1016/j.biortech.2014.02.004

510 Chaker, A., Mutje, P., Vilaseca, F., & Boufi, S. (2013). Reinforcing potential of nanofibrillated cellulose
511 from nonwoody plants. *Polymer Composites*, *34*(12), 1999–2007. https://doi.org/10.1002/pc.22607

512 Chinga-Carrasco, G. (2011). Cellulose fibres, nanofibrils and microfibrils: The morphological sequence
513 of MFC components from a plant physiology and fibre technology point of view. *Nanoscale*
514 *Research Letters*, *6*(1), 417. https://doi.org/10.1186/1556-276X-6-417

515 Chiriac, A. I., Cadena, E. M., Vidal, T., Torres, A. L., Diaz, P., Javier Pastor, F. I., & Pastor, F. I. J.
516 (2010). Engineering a family 9 processive endoglucanase from *Paenibacillus barcinonensis*
517 displaying a novel architecture. *Applied Microbiology and Biotechnology*, *86*(4), 1125–1134.
518 https://doi.org/10.1007/s00253-009-2350-8

519 Czaja, W., Romanovicz, D., & Brown Jr, R. M. (2004). Structural investigations of microbial cellulose
520 produced in stationary and agitated culture. *Cellulose*, *11*(3/4), 403–411.
521 https://doi.org/10.1023/B:CELL.0000046412.11983.61

522 Davidson, G. F. (1948). 6—THE ACIDIC PROPERTIES OF COTTON CELLULOSE AND DERIVED

OXYCELLULOSES. Part II. THE ABSORPTION OF METHYLENE BLUE. *Journal of the Textile Institute Transactions*, *39*(3), T65–T86. https://doi.org/10.1080/19447024808659403

Delgado-Aguilar, M., González Tovar, I., Tarrés, Q., Alcalá, M., Pèlach, M. À., & Mutjé, P. (2015). Approaching a Low-Cost Production of Cellulose Nanofibers for Papermaking Applications. *BioResources*, *10*(3), 5345–5355. https://doi.org/10.15376/biores.10.3.5345-5355

Eibinger, M., Sattelkow, J., Ganner, T., Plank, H., & Nidetzky, B. (2017a). Single-molecule study of oxidative enzymatic deconstruction of cellulose. *Nature Communications*, *8*(1), 894. https://doi.org/10.1038/s41467-017-01028-y

Eibinger, M., Sattelkow, J., Ganner, T., Plank, H., & Nidetzky, B. (2017b). Single-molecule study of oxidative enzymatic deconstruction of cellulose. *Nature Communications*, *8*(1), 894. https://doi.org/10.1038/s41467-017-01028-y

Fillat, Ú., Wicklein, B., Martín-Sampedro, R., Ibarra, D., Ruiz-Hitzky, E., Valencia, C., … Eugenio, M. E. (2018). Assessing cellulose nanofiber production from olive tree pruning residue. *Carbohydrate Polymers*, *179*, 252–261. https://doi.org/10.1016/J.CARBPOL.2017.09.072

Forsberg, Z., Røhr, Å. K., Mekasha, S., Andersson, K. K., Eijsink, V. G. H., Vaaje-Kolstad, G., … Sørlie, M. (2014). Comparative study of two chitin-active and two cellulose-active AA10-type lytic polysaccharide monooxygenases. *Biochemistry*, *53*(10), 1647–56. https://doi.org/10.1021/bi5000433

Frommhagen, M., Mutte, S. K., Westphal, A. H., Koetsier, M. J., Hinz, S. W. A., Visser, J., … Kabel, M. A. (2017). Boosting LPMO-driven lignocellulose degradation by polyphenol oxidase-activated lignin building blocks. *Biotechnology for Biofuels*, *10*(1), 121. https://doi.org/10.1186/s13068-017-0810-4

Garcia-Ubasart, J., Torres, A. L., Vila, C., Pastor, F. I. J., & Vidal, T. (2013). Biomodification of cellulose flax fibers by a new cellulase. *Industrial Crops and Products*, *44*, 71–76. https://doi.org/10.1016/J.INDCROP.2012.10.019

Ghatge, S. S., Telke, A. A., Waghmode, T. R., Lee, Y., Lee, K.-W., Oh, D.-B., … Kim, S.-W. (2015). Multifunctional cellulolytic auxiliary activity protein HcAA10-2 from Hahella chejuensis enhances enzymatic hydrolysis of crystalline cellulose. *Applied Microbiology and Biotechnology*, *99*(7), 3041–55. https://doi.org/10.1007/s00253-014-6116-6

Hall, M., Bansal, P., Lee, J. H., Realff, M. J., & Bommarius, A. S. (2010). Cellulose crystallinity - a

key predictor of the enzymatic hydrolysis rate. *FEBS Journal*, *277*(6), 1571–1582. https://doi.org/10.1111/j.1742-4658.2010.07585.x

Hu, J., Arantes, V., Pribowo, A., Gourlay, K., & Saddler, J. N. (2014). Substrate factors that influence the synergistic interaction of AA9 and cellulases during the enzymatic hydrolysis of biomass. *Energy & Environmental Science*, *7*(7), 2308. https://doi.org/10.1039/c4ee00891j

Hu, J., Tian, D., Renneckar, S., & Saddler, J. N. (2018). Enzyme mediated nanofibrillation of cellulose by the synergistic actions of an endoglucanase, lytic polysaccharide monooxygenase (LPMO) and xylanase. *Scientific Reports*, *8*(1), 3195. https://doi.org/10.1038/s41598-018-21016-6

Iwamoto, S., Abe, K., & Yano, H. (2008). The Effect of Hemicelluloses on Wood Pulp Nanofibrillation and Nanofiber Network Characteristics. *Biomacromolecules*, *9*(3), 1022–1026. https://doi.org/10.1021/bm701157n

Johansen, K. S. (2016a). Discovery and industrial applications of lytic polysaccharide mono-oxygenases. *Biochemical Society Transactions*, *44*(1), 143–149. https://doi.org/10.1042/BST20150204

Johansen, K. S. (2016b). Lytic Polysaccharide Monooxygenases: The Microbial Power Tool for Lignocellulose Degradation. *Trends in Plant Science*, *21*(11), 926–936. https://doi.org/10.1016/j.tplants.2016.07.012

Karim, Z., Afrin, S., Husain, Q., & Danish, R. (2017). Necessity of enzymatic hydrolysis for production and functionalization of nanocelluloses. *Critical Reviews in Biotechnology*, *37*(3), 355–370. https://doi.org/10.3109/07388551.2016.1163322

Lo Leggio, L., Simmons, T. J., Poulsen, J.-C. N., Frandsen, K. E. H., Hemsworth, G. R., Stringer, M. A., … Walton, P. H. (2015). Structure and boosting activity of a starch-degrading lytic polysaccharide monooxygenase. *Nature Communications*, *6*(1), 5961. https://doi.org/10.1038/ncomms6961

Lombard, V., Golaconda Ramulu, H., Drula, E., Coutinho, P. M., & Henrissat, B. (2014). The carbohydrate-active enzymes database (CAZy) in 2013. *Nucleic Acids Research*, *42*(Database issue), D490-495. https://doi.org/10.1093/nar/gkt1178

Miller, G. L. (1959). Use of Dinitrosalicylic Acid Reagent for Determination of Reducing Sugar. *Analytical Chemistry*, *31*(3), 426–428. https://doi.org/10.1021/ac60147a030

Missoum, K., Belgacem, M., & Bras, J. (2013). Nanofibrillated Cellulose Surface Modification: A Review. *Materials*, *6*(5), 1745–1766. https://doi.org/10.3390/ma6051745

Moser, F., Irwin, D., Chen, S., & Wilson, D. B. (2008). Regulation and characterization ofThermobifida

583 fusca carbohydrate-binding module proteins E7 and E8. *Biotechnology and Bioengineering*, *100*(6),
584 1066–1077. https://doi.org/10.1002/bit.21856
585 Nakagawa, Y. S., Eijsink, V. G. H., Totani, K., & Vaaje-Kolstad, G. (2013). Conversion of α-Chitin
586 Substrates with Varying Particle Size and Crystallinity Reveals Substrate Preferences of the
587 Chitinases and Lytic Polysaccharide Monooxygenase of *Serratia marcescens*. *Journal of*
588 *Agricultural and Food Chemistry*, *61*(46), 11061–11066. https://doi.org/10.1021/jf402743e
589 Pääkkö, M., Ankerfors, M., Kosonen, H., Nykänen, A., Ahola, S., Österberg, M., … Lindström, T.
590 (2007). Enzymatic Hydrolysis Combined with Mechanical Shearing and High-Pressure
591 Homogenization for Nanoscale Cellulose Fibrils and Strong Gels. *Biomacromolecules*, *8*(6), 1934–
592 1941. https://doi.org/10.1021/bm061215p
593 Park, S., Baker, J. O., Himmel, M. E., Parilla, P. A., & Johnson, D. K. (2010). Cellulose crystallinity
594 index: measurement techniques and their impact on interpreting cellulase performance.
595 *Biotechnology for Biofuels*, *3*(1), 10. https://doi.org/10.1186/1754-6834-3-10
596 Saito, T., Kimura, S., Nishiyama, Y., & Isogai, A. (2007). Cellulose Nanofibers Prepared by TEMPO-
597 Mediated Oxidation of Native Cellulose. https://doi.org/10.1021/BM0703970
598 Saito, T., Nishiyama, Y., Putaux, J.-L., Vignon, M., & Isogai, A. (2006). Homogeneous Suspensions of
599 Individualized Microfibrils from TEMPO-Catalyzed Oxidation of Native Cellulose.
600 *Biomacromolecules*, *7*(6), 1687–1691. https://doi.org/10.1021/bm060154s
601 Segal, L., Creely, J. J., Martin, A. E., & Conrad, C. M. (1959). An Empirical Method for Estimating the
602 Degree of Crystallinity of Native Cellulose Using the X-Ray Diffractometer. *Textile Research*
603 *Journal*, *29*(10), 786–794. https://doi.org/10.1177/004051755902901003
604 Shatkin, J. A., Wegner, T. H., Bilek, E. M. (Ted), & Cowie, J. (2014). Market projections of cellulose
605 nanomaterial-enabled products- Part 1: Applications. *TAPPI JOURNAL, Volume 13, Number 5,*
606 *2014; Pp. 9-16.*, *13*(5), 9–16. Retrieved from https://www.fs.usda.gov/treesearch/pubs/46174
607 Spence, K. L., Venditti, R. A., Rojas, O. J., Habibi, Y., & Pawlak, J. J. (2011). A comparative study of
608 energy consumption and physical properties of microfibrillated cellulose produced by different
609 processing methods. *Cellulose*, *18*(4), 1097–1111. https://doi.org/10.1007/s10570-011-9533-z
610 Vaaje-Kolstad, G., Forsberg, Z., Loose, J. S., Bissaro, B., & Eijsink, V. G. (2017). Structural diversity of
611 lytic polysaccharide monooxygenases. *Current Opinion in Structural Biology*, *44*, 67–76.
612 https://doi.org/10.1016/J.SBI.2016.12.012

Vaaje-Kolstad, G., Westereng, B., Horn, S. J., Liu, Z., Zhai, H., Sørlie, M., … Eijsink, V. G. H. (2010). An oxidative enzyme boosting the enzymatic conversion of recalcitrant polysaccharides. *Science (New York, N.Y.)*, *330*(6001), 219–22. https://doi.org/10.1126/science.1192231

Valenzuela, S. V., Ferreres, G., Margalef, G., & Pastor, F. I. J. (2017). Fast purification method of functional LPMOs from Streptomyces ambofaciens by affinity adsorption. *Carbohydrate Research*, *448*, 205–211. Retrieved from http://www.sciencedirect.com/science/article/pii/S0008621517300770

Vermaas, J. V., Crowley, M. F., Beckham, G. T., & Payne, C. M. (2015). Effects of Lytic Polysaccharide Monooxygenase Oxidation on Cellulose Structure and Binding of Oxidized Cellulose Oligomers to Cellulases. *The Journal of Physical Chemistry B*, *119*(20), 6129–6143. https://doi.org/10.1021/acs.jpcb.5b00778

Villares, A., Moreau, C., Bennati-Granier, C., Garajova, S., Foucat, L., Falourd, X., … Cathala, B. (2017). Lytic polysaccharide monooxygenases disrupt the cellulose fibers structure. *Scientific Reports*, *7*, 40262. https://doi.org/10.1038/srep40262

Westereng, B., Agger, J. W., Horn, S. J., Vaaje-Kolstad, G., Aachmann, F. L., Stenstrøm, Y. H., & Eijsink, V. G. H. H. (2013). Efficient separation of oxidized cello-oligosaccharides generated by cellulose degrading lytic polysaccharide monooxygenases. *Journal of Chromatography A*, *1271*(1), 144–152. https://doi.org/10.1016/j.chroma.2012.11.048

Westereng, B., Arntzen, M. Ø., Agger, J. W., Vaaje-Kolstad, G., & Eijsink, V. G. H. (2017). Analyzing Activities of Lytic Polysaccharide Monooxygenases by Liquid Chromatography and Mass Spectrometry (pp. 71–92). https://doi.org/10.1007/978-1-4939-6899-2_7

Wood, T. M. (1988). Preparation of crystalline, amorphous, and dyed cellulase substrates. In *Methods in Enzymology* (Vol. 160, pp. 19–25). https://doi.org/10.1016/0076-6879(88)60103-0

Zhang, Y.-H. P., Cui, J., Lynd, L. R., & Kuang, L. R. (2006). A transition from cellulose swelling to cellulose dissolution by *o*-phosphoric acid: Evidence from enzymatic hydrolysis and supramolecular structure. *Biomacromolecules*, *7*(2), 644–648. https://doi.org/10.1021/bm050799c

Zhang, Y.-H. P., & Lynd, L. R. (2006). A functionally based model for hydrolysis of cellulose by fungal cellulase. *Biotechnology and Bioengineering*, *94*(5), 888–898. https://doi.org/10.1002/bit.20906

Supplementary data

Click here to download Supplementary data: SI 2.pptx